Icosahedral-Decahedral Transformation in the $(PdAg)_{309}$ Cluster Induced by Ag Atomic Segregation

Guojian Li[1], Qiang Wang[1], Yongze Cao[1], Kai Wang[1] Jiaojiao Du[1] and Jicheng He[1]

Abstract: This paper studies the influence of Ag atomic segregation on the structural evolutions of the mixed $(PdAg)_{309}$ clusters during the heating processes by using molecular dynamics with a general embedded atom method. The results show that the Ag atomic segregation makes the cluster exhibit a segregate-melting stage in which the energy does not monotonic increase with the increase of temperature. In this stage, the cluster first transforms to form a disorder structure from the initial icosahedron and then a decahedron. By comparing with the cases in the pure Pd_{309}, Ag_{309}, and core-shell $(PdAg)_{309}$, it is found that the icosahedral-decahedral transformation is induced by the Ag atomic segregation.

Keywords: Bimetallic cluster, segregation, structure, Molecular dynamics simulation.

1 Introduction

Specific chemical and physical properties of bimetallic clusters have led to widespread applications in catalysts, sensors, microelectronic and optoelectronic devices [Ferrando et al. (2008)]. Structure, composition, and segregation play a key role in determining these properties especially for catalytic activity [Mainardi and Balbuena (2001); Molenbroek et al. (1998)]. Therefore, interest arises in the study of the effect of composition and segregation during the thermodynamic and interaction processes on the structure of bimetallic cluster [Chushak and Bartell (2003); Mariscal et al. (2005); Kim et al. (2008); Calvo et al. (2008); Rossi and Ferrando (2007)].

Surface energies are different for different elements [Nanda et al. (2002)]. This leads to different atomic behaviors in bimetallic clusters during the thermodynamic

---

[1] Key Laboratory of Electromagnetic Processing of Materials (Ministry of Education), Northeastern University, Shenyang 110819, China. Email: wangq@mail.neu.edu.cn.

and formation processes. Generally, there are several aspects should be considered. The first is the thermodynamic effect. For instance, the melting point can be tuned by selectively doping [Motte et al. (2005)]. An irregular phenomenon of melting, which the atomic energy decreases with the increase of temperature, can be induced by Cu atomic segregation in the Co-Cu-Co onion-like structure [Li et al. (2010)]. The second is that bimetallic clusters present various chemical orderings, such as core-shell, onion-like, and Janus-like [Parsina and Baletto (2010)]. Thirdly, the structure can be influenced. The structure of cluster was generally formed by the surface-induced or surface reconstruction mechanism [Nam et al. (2002); Rodriguez-Lopez et al. (2004)]. Therefore, the surface layer formed by hetero atoms can affect the structure of bimetallic cluster. A Co-Ag core-shell structure with an hcp-like core was formed by the frozen Co-Ag cluster [Dorfbauer et al. (2006)]. The temperature of martensitic transformation for Ag-Au cluster was clearly decreased by constructing a core-shell Au-Ag structure with Ag atoms coating on the Au core [Chen and Johnston (2008)]. In our previous study of the coalescence of clusters Co and Cu [Li et al. (2008)], the coating layer formed by Cu atoms on the Co cluster can make the coalesced complex form fcc, or twined fcc and hcp structure.

All the results indicated that the structure of the cluster was affected by the hetero coating layer on bimetallic cluster. In fact, the atoms with a low surface energy preferably segregate to the surface layer of bimetallic cluster. The segregation process results in not only forming a coating layer but also existing the dynamics behavior of atomic segregation. Both of them can influence the structural formation of bimetallic cluster. Similar segregation phenomena always exist during the fabrication of alloy nanoparticle by using physical vapor deposition method [Binns (2001)]. Furthermore, the experimental results indicated that the formation of decahedral structure in bimetallic cluster was easier than that of icosahedron [Stappert et al. (2003); Tan et al. (2006); Pauwels et al. (2001)] even though the latter has the lowest free energy. Therefore, research on the influence of atomic segregation on the structural evolution plays a key role in studying above-mentioned phenomenon and exploring new nanostructural material. However, very little is known about the influence of atomic segregation on the structural transformation. An understanding as to why the formation of a decahedron occurs so frequently in experiment is also still lacking. All these should be further studied.

The objective of this study is to investigate the influence of atomic segregation on the structural variation during the heating process. Since Ag has a low surface energy, $\sigma(111)_{Ag}$=59.8 kJ/mol, than Pd, $\sigma(111)_{Pd}$=85.9 kJ/mol [Zhu and DePristo (1997)], Ag atoms are more likely to segregate to the surface layer of Pd-Ag cluster. The Pd-Ag cluster including 309 atoms $(PdAg)_{309}$ were selected as the model

materials. Molecular dynamics simulation with an embedded atom method (EAM) was used to study the heating process. The energy-temperature curve, atomic distribution, bond order parameter W_6 [Sankaranarayanan et al. (2005); Cheng and Cao (2008)], and snapshot were used to analyze the structural evolution. In order to define the Ag atomic segregation, the melting of core-shell (PdAg)$_{309}$ with a same Ag concentration, and pure Ag$_{309}$ and Pd$_{309}$ clusters was also calculated to compare with the case of the mixed (PdAg)$_{309}$.

2   Simulation details

All the clusters in this study include 309 atoms. According to previous studies [Li et al. (2009a)], the structural transformation of the cluster is dependent on the release of excess energy. For the Pd-Ag cluster including 309 atoms, a large released excess energy can be induced by Ag atomic segregation. The structural transformation is easily induced by the released excess energy. Then, pure Ag$_{309}$ and Pd$_{309}$ clusters with icosahedral structure were constructed. The mixed (PdAg)$_{309}$ cluster with 93 Ag atoms was obtained by randomly substituting 93 Pd atoms with Ag atoms in Pd$_{309}$. The mixed cluster is that the Ag and Pd atoms are mixed randomly in the cluster. The atomic distributions along the radius direction are shown in Fig. 1. It can be seen from the peaks that there are five layers from core to surface. For the mixed cluster, Ag and Pd atoms are presented in each layer except for the first layer, which has only one atom exist. The core-shell structure consists of a shell of one type of atom (Ag) surrounding a core of another the other (Pd). The core-shell (PdAg)$_{309}$ was setup by randomly substituting 93 Pd atoms only on the Pd$_{309}$ surface layer with Ag atoms. From Fig. 1, all the Ag atoms distribute on the surface layer (5th layer) and form the Ag shell. In Pd-Ag clusters, the Ag atomic segregation is strongly related to Ag contents [Li et al. (2012)]. The cluster with a small Ag content can not release enough energy to induce structural transformation. However, if Ag content is large, not all the Ag atoms segregate to the surface, Ag-Pd-Ag onion-like structure would be formed. The lattice misfit of the interface between Ag and Pd atomic layers will make the cluster form a disorder structure. Therefore, there is a content threshold. 30% Ag content is an effective content, that all the Ag atoms can segregate to the surface to avoid form disorder cluster and also induce a structural transformation. Therefore, the concentration with 93 Ag atoms (30% Ag) was selected. Then, these clusters were relaxed for 0.5 ns at 300 K to obtain the initial cluster.

The simulation method used in this study and its accuracy in simulating bimetallic cluster have been described in our previous studies [Li et al. (2008, 2009b)]. The EAM potential was used as the interatomic force. The potential assumes that the crystal energy is the sum of a pair energy and an embedding energy which is
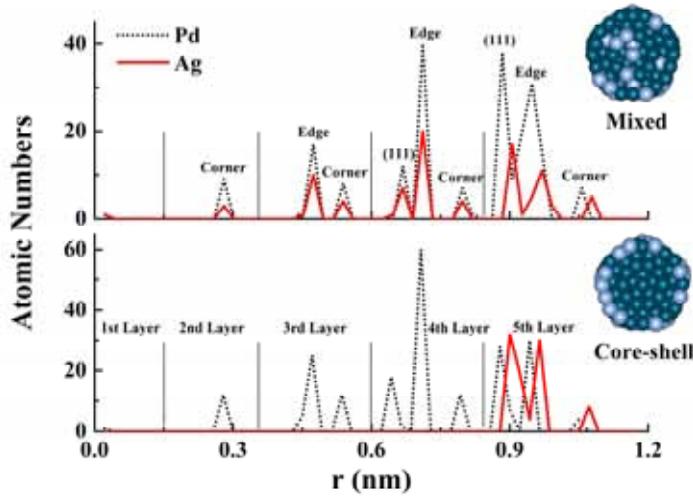
Figure 1: Atomic number along the radius direction for the mixed and core-shell (PdAg)$_{309}$ after the cluster relaxed for 0.5 ns at 300 K. The sphere is the cross section of the cluster. The Pd atom is represented by dark blue and the Ag atom by light blue

required to embed an atom into a local medium with a given electron density. In EAM, the total energy E of the crystal can be expressed as

$$E = \frac{1}{2} \sum_{i,j,i\neq j} \phi_{ij}(r_{ij}) + \sum_i F_i(\rho_i), \tag{1}$$

where $\phi_{ij}(r_{ij})$ is the pair energy between atoms i and j separated by r_{ij}, and $F_i(\rho_i)$ is the embedding energy to embedded an atom i into an electron density ρ_i. ρ_i can be calculated using

$$\rho_i = \sum_{j(j\neq i)} f_j(r_{ij}), \tag{2}$$

where $f_j(r_{ij})$ is the electron density at the i atomic site arising by j atom at a distance of r_{ij}. It can be written as

$$f(r) = \frac{f_e \exp[-\beta(\frac{r}{r_e}-1)]}{1+(\frac{r}{r_e}-\lambda)^{20}}, \tag{3}$$

where f_e is scaling factors, for pure metal, $f_e = 1$. For alloy, $f_e = (E_C/\Omega)^{\gamma_1}$. r_e is the equilibrium spacing between nearest neighboring atoms.

The generalized pair potentials have the form

$$\phi(r) = \frac{A \cdot \exp[-\alpha(\frac{r}{r_e} - 1)]}{1 + (\frac{r}{r_e} - \kappa)^{20}} - \frac{B \cdot \exp[-\beta(\frac{r}{r_e} - 1)]}{1 + (\frac{r}{r_e} - \lambda)^{20}}. \tag{4}$$

$A, B, \alpha, \beta, \kappa,$ and λ are adjustable parameters. For the alloy model, the pair potential between different species a and b is defined by using the alloy model proposed by Johnson [Johnson (1990)]

$$\phi^{ab}(r) = \frac{1}{2}\left(\frac{f^b(r)}{f^a(r)}\phi^{aa}(r) + \frac{f^a(r)}{f^b(r)}\phi^{bb}(r)\right). \tag{5}$$

In order to make the embedding energy functions work well over a wide range of electron density, the embedding energy functions are divided as three equations:

$$F(\rho) = \begin{cases} \sum\limits_{i=0}^{3} F_{ni}(\frac{\rho}{\rho_n} - 1)^i, & \rho < \rho_n,\ \rho_n = 0.85\rho_e \\ \sum\limits_{i=0}^{3} F_i(\frac{\rho}{\rho_e} - 1)^i, & \rho_n \leq \rho < \rho_o, \rho_o = 1.15\rho_e \\ F_e\left[1 - \ln\left(\frac{\rho}{\rho_e}\right)^\eta\right] \cdot \left(\frac{\rho}{\rho_e}\right)^\eta, & \rho_o \leq \rho \end{cases} \tag{6}$$

With this model, the parameters can be found in Ref. 29.

The time step was 1 fs. The thermodynamic process was simulated as follows. (1) The cluster was heated up to 900 K from 300 K with 20 K temperature step and 0.5 ns time step. (2) The cluster was heated up to 1200 K from 900 K with 50 K temperature step and 0.5 ns time step.

3 Results and discussion

Fig. 2 gives the temperature dependence of the atomic potential energy in the mixed and core-shell (PdAg)₃₀₉ and the Ag atomic number in the inner of the mixed (PdAg)₃₀₉. The melting points of both clusters are same (780 K). The potential energies in both clusters are almost same with the increase of temperature after the clusters melted. However, their energy-temperature curves are obviously different before the clusters melting. The energy of the mixed (PdAg)₃₀₉ is higher than that of the core-shell (PdAg)₃₀₉ at the same temperature. This is because Ag has a lower surface energy than that of Pd, the distribution of Ag atoms on the surface layer decreases the potential energy of the core-shell (PdAg)₃₀₉. In addition, the atomic potential energy does not monotonously increase with the increase of temperature from 580 to 760 K. By observing the Ag atomic number in the inner in Fig. 2, it can be found that this strongly relates to the decrease of the Ag atomic number.

In other words, the Ag segregation from the inner to the surface layer results in the phenomenon. In this study, this stage hereafter is called as "segregate-melting stage". This is similar to the results of our previous study that the atomic energy decreases with the increase of temperature in the Cu-Co cluster [Li et al. (2010)]. But there are some differences. In our previous study, the atomic energy decreases with the increase of temperature due to the Cu segregation. Here, the potential energy increases from 660 to 680 K in spite of the occurrence of Ag atomic segregation. This is because that the appearance of lattice distortion between Pd and Ag makes the cluster change to a disorder state. This leads to the increase of atomic potential energy. In addition, there is no atomic segregation from 700 to 720 K, while the potential energy was decreased with the increase of temperature. There must be a structural transformation that leads to the energy decrease. Then, from 720 to 760 K, there is no atomic segregation, the potential energy was also increased with the increase of temperature. But the atomic energy of the mixed $(PdAg)_{309}$ is higher than that of the core-shell $(PdAg)_{309}$. This may be due to that not all the Ag atoms segregated to the surface layer. Finally, all the Ag atoms segregate to the surface layer after the cluster melted.
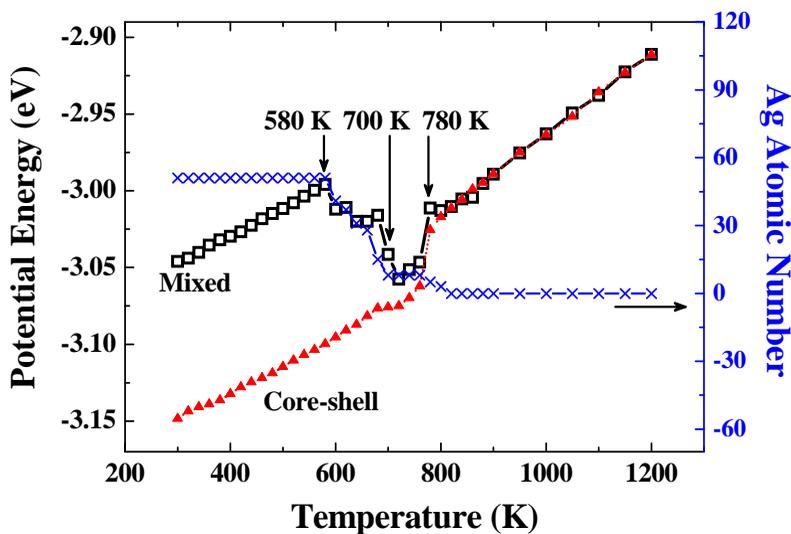
Figure 2: Temperature dependence of the atomic potential energy and the Ag atomic number in the inner of the mixed and core-shell $(PdAg)_{309}$ clusters

The bond order parameter W_6 was used to study the structural evolution in the segregate-melting stage of the cluster. In order to exploring the evolution in the

mixed (PdAg)$_{309}$, the W_6 values of the core-shell (PdAg)$_{309}$, pure Pd$_{309}$, and Ag$_{309}$ were also calculated, as shown in Fig. 3. In addition, the standard W_6 values of liquid, icosahedron and decahedron are also depicted in dot lines in the figure. The W_6 values of all the clusters in the initial stage are near the icosahedral value due to their initial icosahedral structure. After the clusters melted, the W_6 values sharply fluctuate in the liquid value. In this study, since the structure used to calculate the W_6 value is an instantaneous structure after relaxed for 0.5 ns at the corresponding temperature, there are a few differences between the calculated W_6 and standard value. For the clusters of the core-shell (PdAg)$_{309}$, pure Pd$_{309}$, and Ag$_{309}$, their W_6 values were almost unchanged before the clusters melting except for some differences with the initial cases at the surface premelting stage. Furthermore, when these three clusters melted, there is a sharp increase for the W_6 value. In the mixed (PdAg)$_{309}$, the variation of the W_6 is different from other clusters because of the existence of the segregate-melting stage. After 580 K, the lattice distortion induced by the Ag atomic segregation increases and the W_6 value also increases. At 680 and 700 K, the W_6 values almost near the liquid value, this indicates the cluster keeps a disorder state like liquid. At 720 K, the W_6 values decrease sharply to near the decahedral value. The clusters transformed to form a decahedral structure. Since there is surface premelting in the cluster, the W_6 value at 720 K is higher than that of the decahedral value. The cluster keeps decahedral structure until the cluster melted. By comparing with the structural transformation and energy-temperature variation, it is found that the potential energy decrease occurs during the structural transformation process. Since there are some Ag atoms in the inner of the cluster, the mixed (PdAg)$_{309}$ formed an Ag-Pd-Ag onion-like decahedron.

The snapshots of clusters were used to further analyze the structural evolutions, as shown in Fig. 4. In order to confirm the frozen structures of the mixed and core-shell (PdAg)$_{309}$, their structures at 700 K were cooled down to 300 K. Here, 700 K was selected due to the disorder state for the mixed (PdAg)$_{309}$. Therefore, the influence of initial structure on the frozen structure can be ignored. For the core-shell (PdAg)$_{309}$, all the morphologies (bottom row in Fig. 4) are icosahedral structure that formed by a quasispherical shape with 20 (111)-like facets. Furthermore, the structure of the cluster at 300 K cooled down from 700 K is still icosahedral. However, the cases are different for the mixed (PdAg)$_{309}$. Its structure is icosahedral at 300 K, the cluster at 700 K formed a disorder cluster due to the lattice distortion of Ag and Pd. While, at 720 K, the cluster formed a decahedral structure which are composed of five slightly distorted truncated tetrahedral that share a common edge. The cluster keeps decahedral structure at 760 K. At the same time, the structure cooled down to 300 from 700 K is also decahedral. This indicates the frozen structure of the mixed (PdAg)$_{309}$ after segregation occurred is decahedral. These
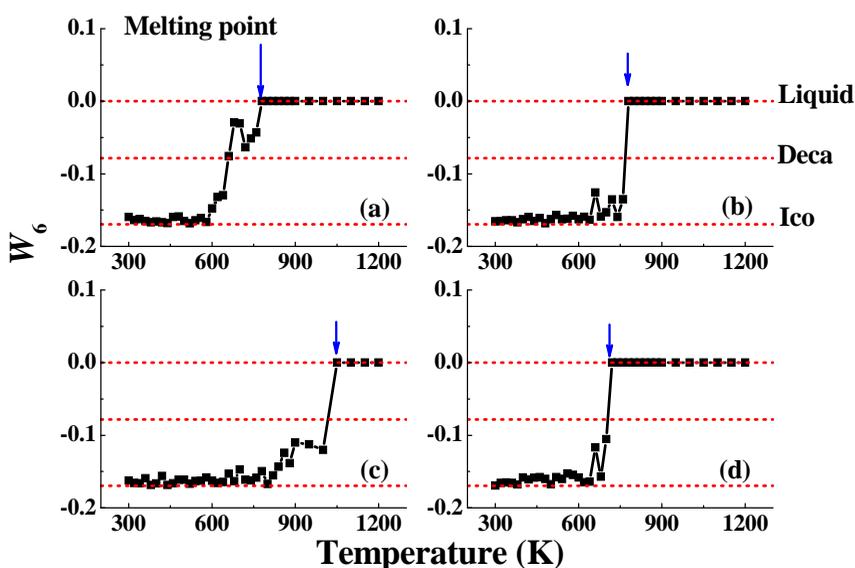
Figure 3: Variation of W_6 for the mixed (a) and core-shell $(PdAg)_{309}$ (b), Pd_{309} (c), and Ag_{309} (d) with temperature.

results are same to those of bond order parameters.

An icosahedral-decahedral structural transformation was occurred in the mixed $(PdAg)_{309}$ but not in the core-shell $(PdAg)_{309}$, pure Pd_{309} and Ag_{309}. It is reasonable to conclude the following results by analyzing all above-mentioned phenomena.

(1) The icosahedral-decahedral transformation occurs only in bimetallic clusters but not in the pure Pd and Ag clusters. This indicates that the transformation was induced by the doping of alloy element and may be tuned by doping with alloy elements.

(2) The transformation occurs in the mixed $(PdAg)_{309}$ but not in the core-shell $(PdAg)_{309}$. The transformation temperature is 720 K. While in this temperature, the Ag coating layer was formed for both clusters. This means that there is no influence of Ag coating layer on the icosahedral-decahedral transformation. The only difference between the mixed and core-shell clusters is the segregating-melting stage (the Ag atomic segregation) during the heating process. This indicates that the Ag atomic segregation leads to the structural transformation.

(3) As above mentioned, the disorder structure of mixed cluster $(PdAg)_{309}$ at 700 K keeps a high energy state. At the same time, the heating process also provides

| Heating 300 K | Heating 700 K | Heating 720 K | Heating 760 K | Cooled down to 300 from 700 K |
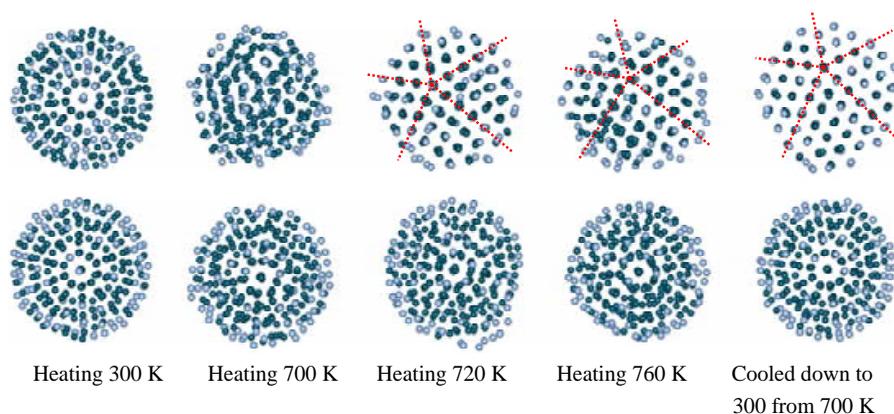
Figure 4: Snapshots of the mixed (top) and core-shell (bottom) (PdAg)$_{309}$ at different temperatures

energy. Therefore, the structural transformation can be driven by both energies. However, if there is no atomic segregation, the decahedral cluster can not be induced. Atomic segregation exists in almost all the bimetallic clusters, therefore, more decahedral structures were found in the experimental research of bimetallic clusters.

4 Conclusions

Molecular dynamics with an EAM potential was used to study the influence of Ag atomic segregation on the melting and structural evolution. Bond order parameter W_6, energy-temperature curve, atomic distribution, and snapshot were used to analyze the variation of energy and structure. In addition, same processes of the pure Pd$_{309}$, Ag$_{309}$, and core-shell (PdAg)$_{309}$ were also studied. A segregate-melting stage appeared in the mixed (PdAg)$_{309}$ during the heating process due to the segregation of Ag from the inner to the surface layer. At this stage, the cluster formed a disorder state (liquid-like) due to the large lattice distortion between Ag and Pd. Then, the disorder cluster transformed to form a decahedral structure with the increase of temperature. These phenomena did not occur in other three clusters. Therefore, the atomic segregation influenced the melting and structure of the clusters. This means that the structure and melting can be tuned by doping with alloy element with different surface energies or concentration, distribution.

References

Binns, C. (2001): Nanoclusters deposited on surfaces. *Surf. Sci. Rep.*, vol. 44, no. 1-2, pp. 1-49.

Calvo, F.; Cottancin, E.; Broyer, M. (2008): Segregation, core alloying, and shape transitins in bimetallic nanoclusters: Monte Carlo simulations. *Phys. Rev. B*, vol. 77, no. 12, pp. 121406(R).

Chen, F. Y.; Johnston, R. L. (2008): Martensitic transformation in Ag-Au bimetallic core-shell nanoalloys. *Appl. Phys. Lett.*, vol. 92, no. 2, pp. 023112.

Cheng, D. J.; Cao, D. P. (2008): Structural transition and melting of onion-ring Pd-Pt bimetallic clusters. *Chem. Phys. Lett.*, vol. 461, no. 1-3, pp. 71-76.

Chushak, Y. G.; Bartell, L. S. (2003): Freezing of Ni-Al bimetallic nanoclusters in computer simulations. *J. Phys. Chem. B*, vol. 107, no. 16, pp. 3747-3751.

Dorfbauer, F.; Schrefl, T.; Kirschner, M.; Hrkac, G.; Suess, D.; Ertl, O.; Fidler, J. (2006): Structure calculation of CoAg core-shell clusters. *J. Appl. Phys.*, vol. 99, no. 8, pp. 08G706.

Ferrando, R.; Jellinek, J.; Johnston, R. L. (2008): Nanoalloys: from theory to applications of alloy clusters and nanoparticles. *Chem. Rev.*, vol. 108, no. 3, pp. 845-910.

Johnson, R. A. (1990): Phase stability of fcc alloys with the embedded-atom method. *Phys. Rev. B*, vol. 41, no. 14, pp. 9717-9720.

Kim, D. H.; Kim, H. Y.; Kim, H. G.; Ryu, J. H.; Lee, H. M. (2008): The solid-to-liquid transition region of an Ag-Pd bimetallic nanocluster. *J. Phys.: Cond. Matt.*, vol. 20, no. 3, pp. 035208.

Li, G. J.; Wang, Q.; Li, D. G.; Lü, X.; He, J. C. (2008): Structure evolution during the cooling and coalesced cooling processes of Cu-Co bimetallic clusters. *Phys. Lett. A*, vol. 372, no. 45, pp. 6764-6769.

Li, G. J.; Wang, Q.; Wang, K.; Liu, T.; Li, D. G.; He, J. C. (2009a): Composition, concentration and configuration dependence of the icosahedral transformations in Cu-based bimetallic clusters. *Model.Simul. Mater. Sc.*, vol. 17, no. 5, pp. 055005.

Li, G. J.; Wang, Q.; Li, D. G.; Lü, X.; He, J. C. (2009b): Size and composition effects on the melting of bimetallic Cu-Ni clusters studied via molecular dynamics simulation. *Mater. Chem. Phys.*, vol. 114, no. 2-3, pp. 746-750.

Li, G. J.; Liu, T.; Wang, Q.; Lü, X.; Wang, K.; He, J. C. (2010): Controllable irregular melting induced by atomic segregation in bimetallic clusters with fabricating different initial configurations. *Phys. Lett. A*, vol. 374, no. 15-16, pp. 1769-1772.

Li, G. J.; Wang, Q.; Liu, T,; Wang, K.; Wu, C.; He, J. C. (2012): Controllable irregular phenomenon induced by Ag atomic segregation on the melting of (AgPd)$_{561}$ bimetallic clusters. *J. Nanopart. Res.*, vol. 14, no. 8, pp. 1068.

Mainardi, D. S.; Balbuena, P. B. (2001): Monte Carlo simulation of Cu-Ni nanoclusters: surface segregation studies. *Langmuir*, vol. 17, no. 6, pp. 2047-2050.

Mariscal, M. M.; Dassie, S. A.; Leiva, E. P. M. (2005): Collision as a way of forming bimetallic nanoclusters of various structre and chemical compositions. Journal of Chemical Physics. *J. Chem. Phys.*, vol. 123, no. 18, pp. 184505.

Molenbroek, A. M.; Haukka, S.; Clausen, B. S. (1998): Alloying in Cu/Pd nanoparticle catalysts. *J. Phys. Chem. B*, vol. 102, no. 52, pp. 10680-10689.

Motte, C.; Rossi, G.; Baletto, F.; Ferrando, R. (2005): Single impurity effect on the melting of nanoclusters. *Phys. Rev. Lett.*, vol. 95, no. 3, pp. 035501.

Nanda, K. K.; Sahu, S. N.; Behera, S. N. (2002): Liquid-drop model for the size-dependent melting of low-dimensional systems. *Phys. Rev. A*, vol. 66, no. 1, pp. 013208.

Nam, H. S.; Hwang, N. M.; Yu, B. D.; Yoon, J. K. (2002): Formation of an icosahedral structure during the freezing of gold nanoclusters: surface-induced mechanism. *Phys. Rev. Lett*, vol. 89, no. 27, pp. 275502.

Parsina, I.; Baletto, F. (2010): Tailoring the structral motif of AgCo nanoalloys: core/shell versus Janus-like. *J. Phys. Chem. C*, vol. 114, no. 3, pp. 1504-1511.

Pauwels, B.; Tendeloo, G. V.; Zhurkin, E.; Hou, M.; Verschoren, G.; Kuhn, T.; Bouwen, W.; Lievens, P. (2001): Transmission electron microscopy and monte carlo simulations of ordering in Au-Cu clusters produced in a laser vaporization source. *Phys. Rev. B*, vol. 63, no. 16, pp. 165406.

Rodriguez-Lopez, J. L.; Montejano-Carrizales, J. M.; Pal, U.; Sanchez-Ramirez, J. F.; Troiani, H. E.; Garcia, D.; Miki-Yoshida, M.; Jose-Yacaman, M. (2004): Surface reconstruction and decahedral structure of bimetallic nanoparticles. *Phys. Rev. Lett.*, vol. 92, no. 19, pp. 196102.

Rossi, G.; Ferrando, R. (2007): Freezing of gold nanoclusters into poly-decahedral structures. *Nanotech.*, vol. 18, no. 22, pp. 225706.

Sankaranarayanan, S. K. R. S.; Bhethanabotla, V. R.; Joseph, B. (2005): Molecular dynamics simulation study of the melting of Pd-Pt nanoclusters. *Phys. Rev. B*, vol. 71, no. 19, pp. 195415.

Stappert, S.; Rellinghaus, B.; Acet, M.; Wassermann, E. F. (2003): Gas-phase preparation of $L1_0$ ordered FePt nanoparticles. *J. Cryst. Growth*, vol. 252, no. 1-3, pp. 440-450.

Tan, C. Y.; Chen, J. S.; Liu, B. H.; Chow, G. M. (2006): Microstructure of FePt nanoparticles produced by nanocluster beam. *J. Cryst. Growth*, vol. 293, no. 1, pp. 175-185.

Zhou, X. W.; Wadley, H. N. G.; Johnson, R. A.; Larson, D. J.; Tabat, N.; Cerezo, A.; Petford-Long, A. K.; Smith, G. D. W.; Clifton, P. H.; Martens, R. L.; Kelly, T. F. (2001): Atomic scale structure of sputtered metal multilayers. Acta Mater., vol. 49, no. 19, pp. 4005-4015.

Zhu, L.; DePristo, A. E. (1997): Microstructures of bimetallic clusters: bond order metal simulator for disordered alloys. *J. Catal.*, vol. 167, no. 2, pp. 400-407.